

Supporting Material

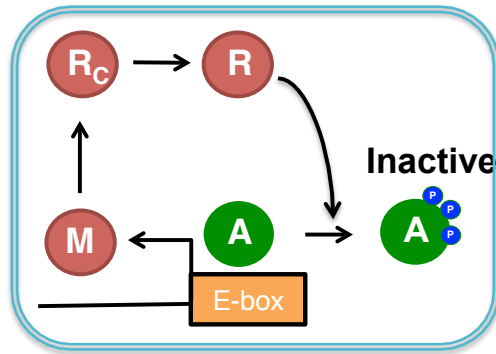
Molecular mechanisms that regulate the coupled period of the mammalian circadian clock

Jae Kyoung Kim¹, Zachary P. Kilpatrick², Matthew R. Bennett^{3,4}, Krešimir Josić^{2,5}

1. Mathematical Biosciences Institute, The Ohio State University, Columbus, OH 43210, USA.
2. Department of Mathematics, University of Houston, Houston, TX 77204-3008.
3. Department of Biochemistry & Cell Biology, Rice University, Houston TX, 77005.
4. Institute of Biosciences and Bioengineering, Rice University, Houston, TX, 77005.
5. Department of Biology and Biochemistry, University of Houston, Houston, TX 77204-5001.

Table of Contents

- **Figure S1.** Phosphorylation-based repression in *Neurospora* circadian clock.....2
- **Figure S2.** mRNA timecourses of PS model and HT model.....3
- **Figure S3.** The coupled periods of two heterogeneous cells with different parameters....4
- **Figure S4.** Coupled periods of two heterogeneous cells via Michaelis-Menten type coupling5
- **Figure S5.** The extended HT model with low Hill coefficient.....6
- **Figure S6.** The coupled periods of 100 heterogeneous cells with a stronger coupling7
- **Figure S7.** The coupled periods of 100 cells with more heterogeneity8
- **Figure S8.** The AIFs with different parameters9
- **Supporting Reference**.....10



- M Repressor mRNA
- Rc Repressor in cytoplasm
- R Repressor in nucleus
- A Activator

Figure S1. Phosphorylation-based repression in *Neurospora* circadian clock. In *Neurospora Crassa* circadian clock, repressor protein (FRQ) recruits kinases that phosphorylate multiple sites of activator protein (WCC). This phosphorylation inactivates the activator protein. Whereas this phosphorylation-based repression is different from the direct repression via oligomerization, which appears in the Goodwin oscillator (Fig. 2B), both mechanisms can be modeled using Hill equations (1). Thus, the Goodwin oscillator has been used as a *Neurospora* circadian clock model (2). The Hill-coefficient represents the number of phosphorylation sites in phosphorylation-based repression mechanism (1).

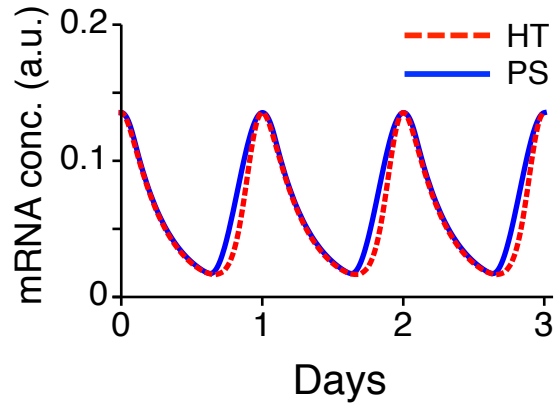


Figure S2. mRNA timecourses of PS model and HT model. Parameters of PS model (K_d and A) and HT model (K_d and n) are selected so the two models have similar amplitudes and periods. Here, $A=0.0659$ and $K_d=10^{-5}$ for PS model and $n=11$ and $K_d=4 \times 10^{-2}$ for HT model.

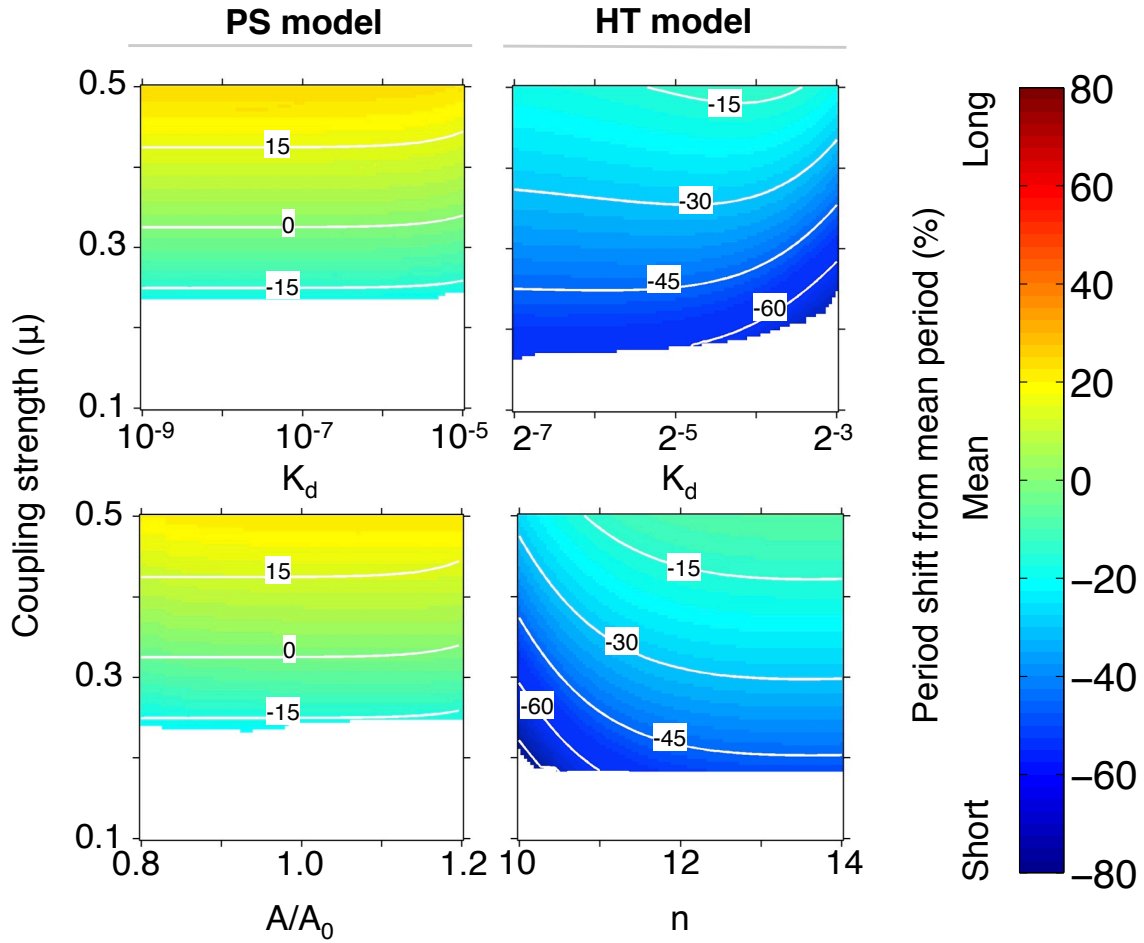


Figure S3. The coupled periods of two heterogeneous cells with different parameters. The shifts of coupled periods from the mean period are represented with color and contour. Regardless of the choice of parameters, the coupled periods of the PS model are similar to the mean period, but those of HT model are shorter than the mean period with a weak coupling ($0.2 < \mu < 0.4$). The coupled periods of HT model are similar to the mean period only when coupling becomes strong ($\mu > 0.5$). Here, A_0 indicates the concentration of activator in the original model. Rescaling factors are 1 and 1.2 for two cells as in Fig. 4A.

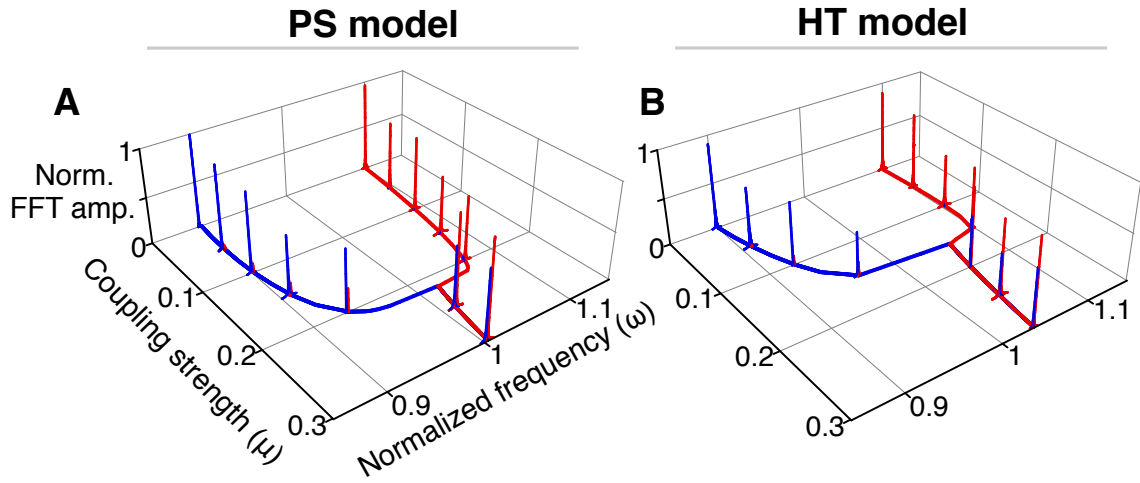


Figure S4. Coupled periods of two heterogeneous cells via Michaelis-Menten type coupling. When Michaelis-Menten type equations were used for coupling, results are similar to Fig. 4A-B, where linear coupling is used.

$$\mu \sum_{i=1}^N V_i / N \rightarrow \frac{\mu \sum_{i=1}^N V_i / N}{K_C + \sum_{i=1}^N V_i / N}$$

Here, $K_C=0.7$ and other parameters were the same with Fig. 4A-B.

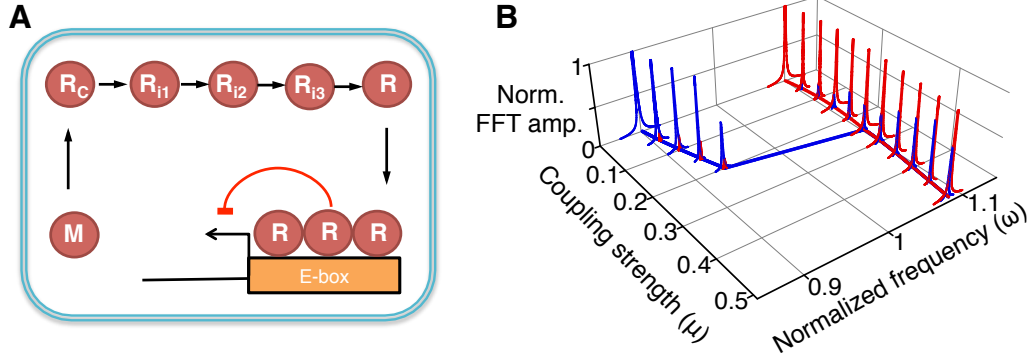


Figure S5. The extended HT model with low Hill coefficient. Three more intermediate steps (R_{i1} , R_{i2} , and R_{i3}) are included between R_C and R of HT model (Fig. 2B), so that the model can oscillate with a Hill coefficient of 3 (3). When a fast cell and a slow cell of the extended model are coupled, the coupled frequency is greater than the mean frequency, as in the original HT model (Fig. 4B). Parameters are the same as Fig. 4B except that Hill-coefficient is reduced to 3. The extended HT model has the form

$$\begin{aligned} \frac{dM}{dt} &= \frac{1}{1 + (R/K_d)^3} - M, \\ \frac{dR_c}{dt} &= M - R_c, \\ \frac{dR_{i1}}{dt} &= R_c - R_{i1}, \\ \frac{dR_{i2}}{dt} &= R_{i1} - R_{i2}, \\ \frac{dR_{i3}}{dt} &= R_{i2} - R_{i3}, \\ \frac{dR}{dt} &= R_{i3} - R. \end{aligned}$$

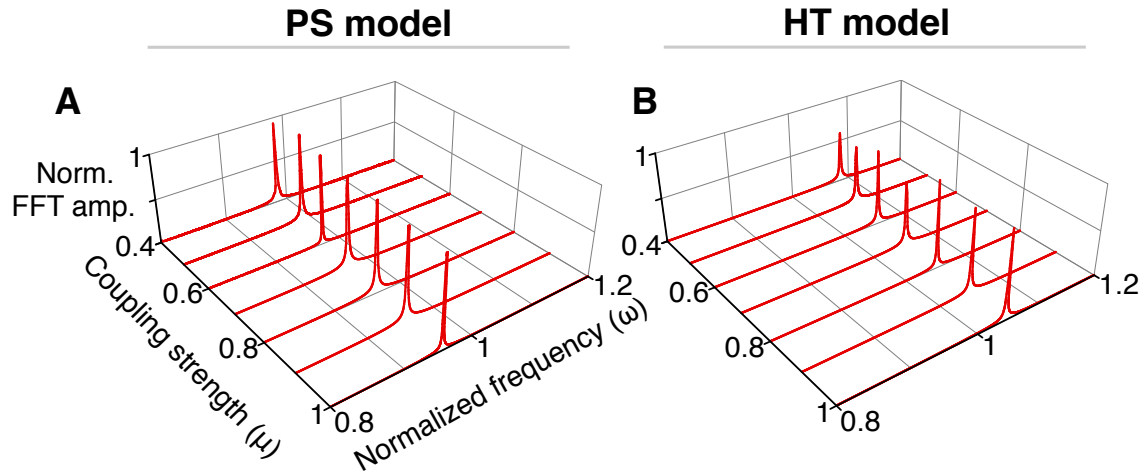


Figure S6. The coupled periods of 100 heterogeneous cells with a stronger coupling. Parameters are the same with Fig. 4C-D except for the coupling strengths.

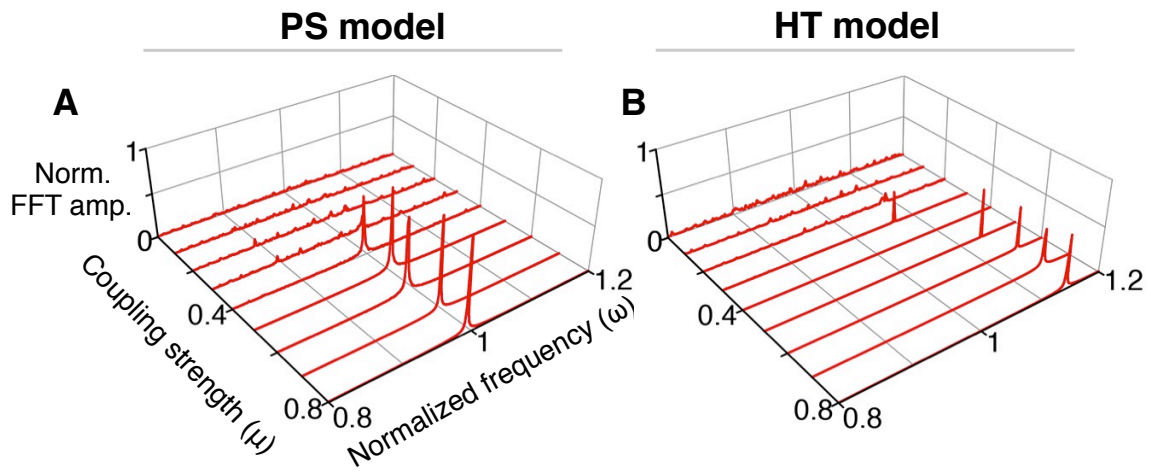


Figure S7. The coupled periods of 100 cells with more heterogeneity. Here, the standard deviation of rescaling factors is 0.2, which is larger than Fig. 4C-D. Other parameters are the same with Fig. 4C-D.

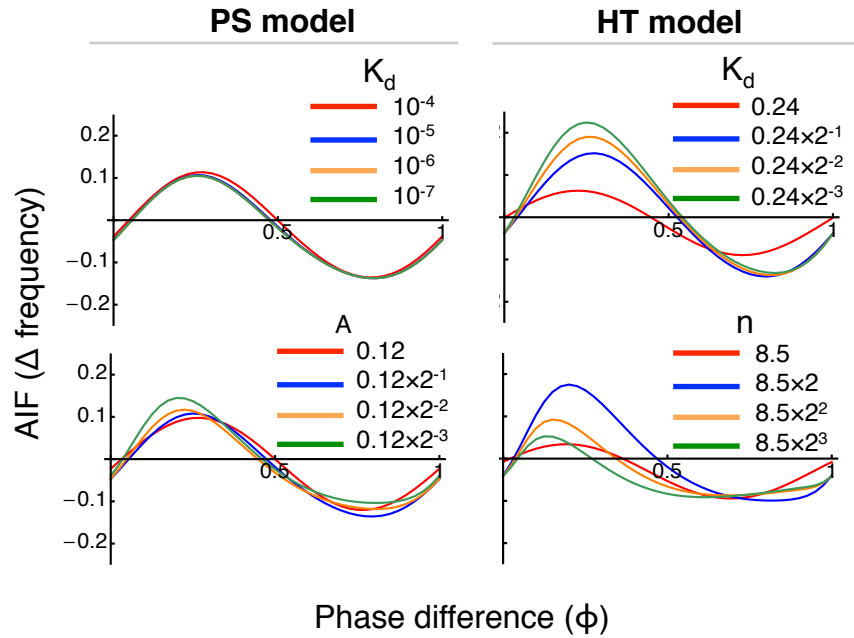


Figure S8. The AIFs with different parameters. Whereas the balanced AIFs of PS models are well maintained over a wide range of parameters, the AIFs of HT model show significant change. Each parameter is perturbed from the value, near which bifurcation occurs and the model begins oscillation.

Supporting Reference

1. Gonze, D., and W. Abou-Jaoudé. 2013. The Goodwin model: behind the Hill function. *PLoS One*. 8: e69573.
2. Ruoff, P., M. Vinsjevik, C. Monnerjahn, and L. Rensing. 2001. The Goodwin model: simulating the effect of light pulses on the circadian sporulation rhythm of *Neurospora crassa*. *J. Theor. Biol.* 209: 29–42.
3. Forger, D.B. 2011. Signal processing in cellular clocks. *Proc. Natl. Acad. Sci. U. S. A.* 108: 4281–4285.